eLIFE elifesciences.org

RESEARCH ARTICLE

Figures and figure supplements

Mechanical stress contributes to the expression of the *STM* homeobox gene in Arabidopsis shoot meristems

Benoît Landrein *et al*

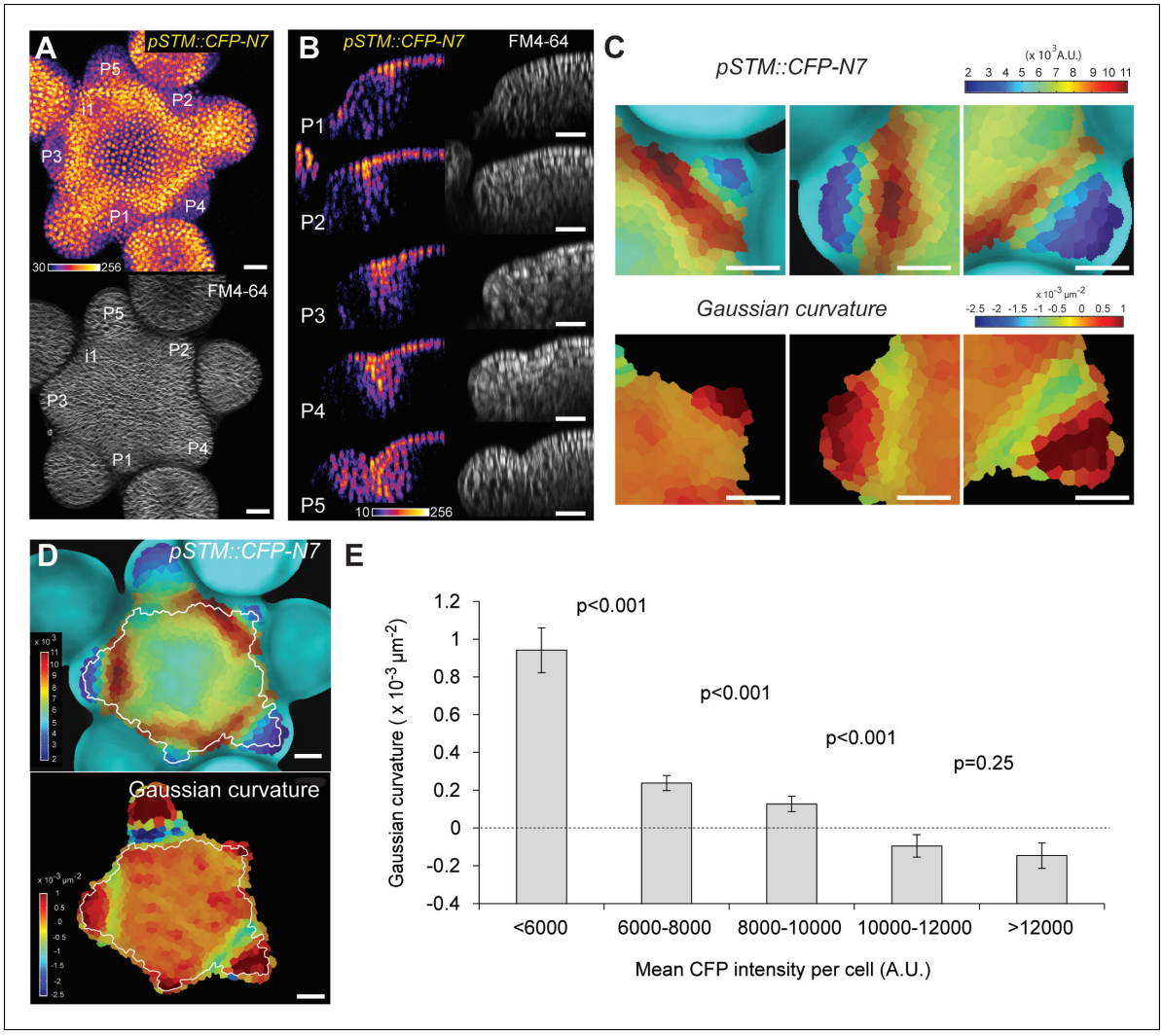

Figure 1. Correlation between *pSTM::CFP-N7* expression level and tissue folding at the boundary. **(A)** *pSTM::CFP-N7* expression pattern in the SAM. Membranes are labeled with FM4-64 (white, lower panel) and *pSTM::CFP-N7* expression is shown using the Fire lookup table in ImageJ (upper panel, n > 20). (**B**) Longitudinal optical sections (5 µm thick maximal projection of orthogonal views) through the middle of five successive boundaries of a representative meristem expressing *pSTM::CFP-N7*. Note the increase of *pSTM::CFP-N7* signal intensity in the boundary as the crease between organ and meristem becomes deeper. **(C)** Close-ups showing a correlation between *pSTM::CFP-N7* signal intensity (upper panels) and Gaussian curvature (lower panels, see Material and methods) in three successive boundaries of the meristem presented in A. (**D and E**) Quantification of the correlation between *pSTM::CFP-N7* signal intensity (upper panel) and Gaussian curvature (lower panel) in the meristem presented in A (see Material and methods). (**D**) The white outline encloses the cells that are used for the graph presented in E. (**E**) *pSTM::CFP-N7* signal intensity is plotted against Gaussian curvature. Values are compared using a bilateral Student test. The same correlation was observed in 5 independent meristems. Scale bars, 20 µm.
DOI: http://dx.doi.org/10.7554/eLife.07811.003

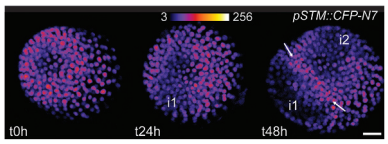

Figure 1—figure supplement 1. Time lapse imaging of a meristem recovering from NPA treatment and expressing *pSTM::CFP-N7*. i1 and i2 marks the presence of new initia where the CFP-N7 signal decreases and the white arrows points toward a new developing boundary where the CFP-N7 signal increases. Note that t = h corresponds to 24 h after transfer to a NPA free medium. Scale bars: 20 μm.
DOI: http://dx.doi.org/10.7554/eLife.07811.004

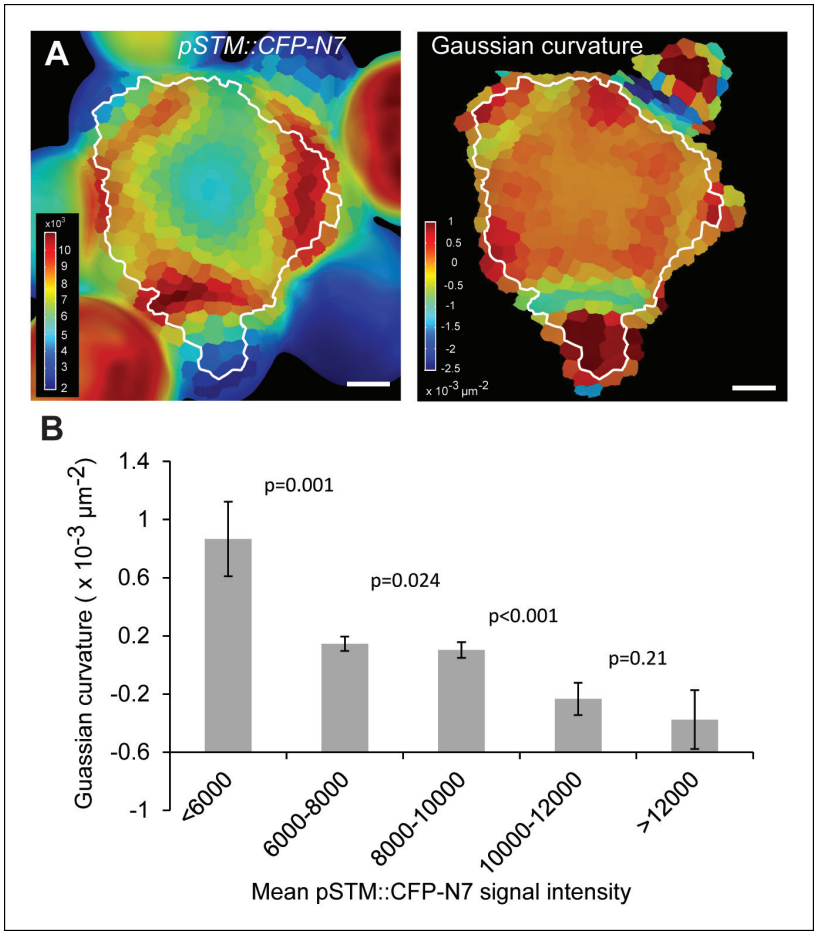

Figure 1—figure supplement 2. Correlation between *pSTM::CFP-N7* expression level and tissue folding at the boundary. (**A**) Correlation between *pSTM::CFP-N7* signal intensity and Gaussian curvature in another meristem than the one presented in ***Figure 1***. The white outline encloses the cells that are used for the graph presented in B (See Material and methods). (**B**) Quantitative measurement of the negative correlation between *pSTM::CFP-N7* intensity and Gaussian curvature in the meristem presented in A (n = 231 cells). Successive values are displayed with a Student confidence interval ($\alpha = 0.05$) and compared using a bilateral Student test. Scale bars: 20 µm.
DOI: http://dx.doi.org/10.7554/eLife.07811.005

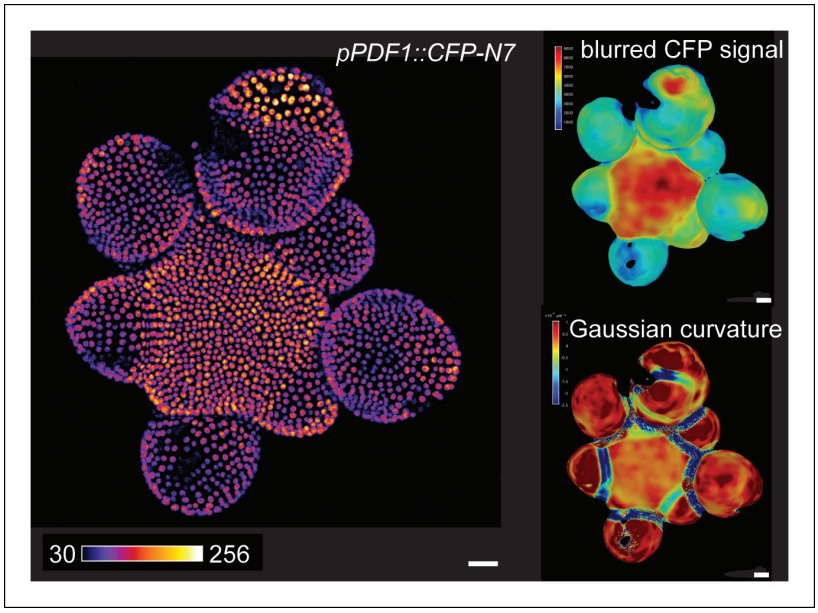

Figure 1—figure supplement 3. *pPDF1::CFP-N7* expression pattern in the SAM. Z-projection of a meristem expressing the L1 transcriptional reporter *pPDF1::CFP-N7* (left panel). CFP-N7 Signal intensity map of the signal and Gaussian curvature extracted using the level set method and MorphoGraphX (right panels). Scale bars: 20 μm.
DOI: http://dx.doi.org/10.7554/eLife.07811.006

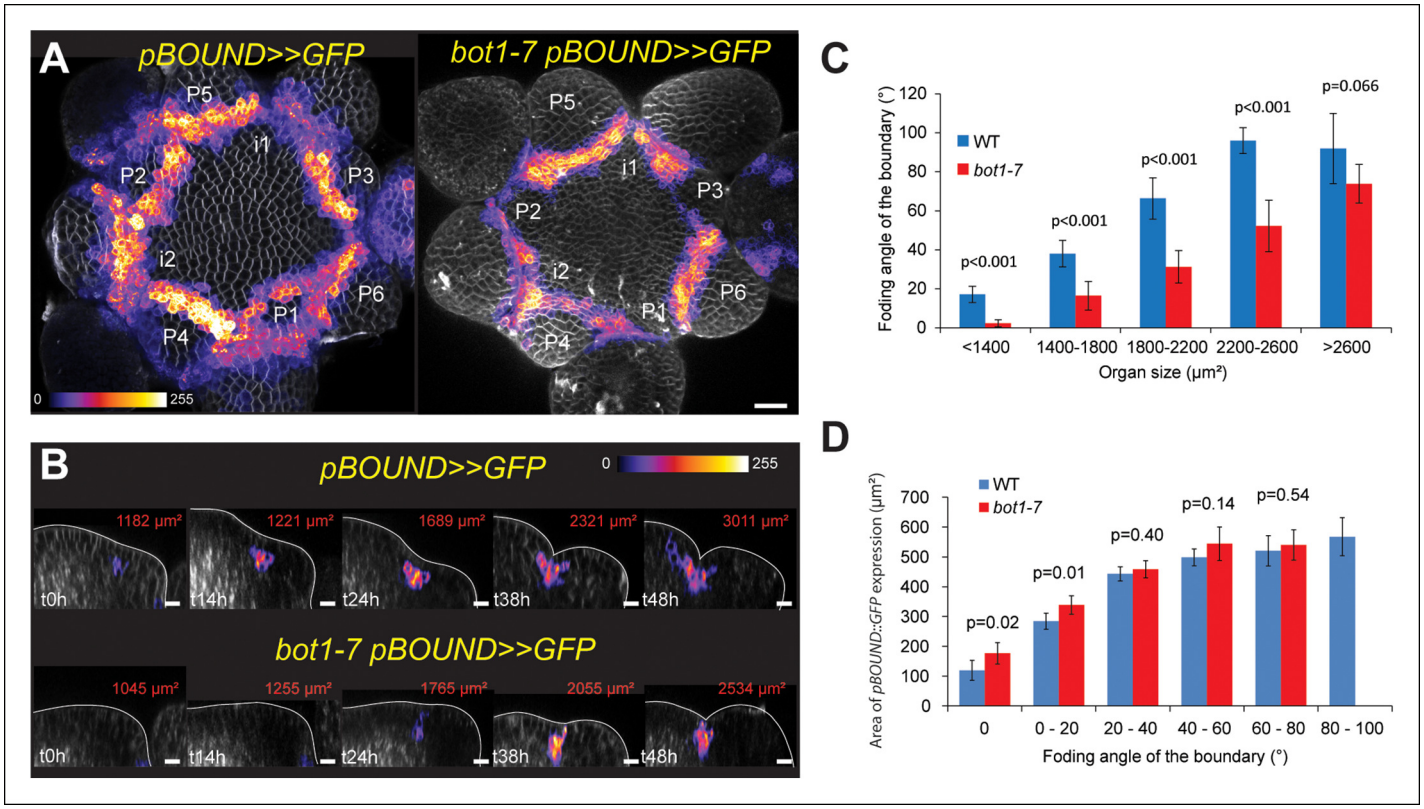

Figure 2. Correlation between *pBOUND>>GFP* expression level and tissue folding at the boundary in WT and *bot1-7*. (**A**) *pBOUND>>GFP* expression pattern in WT (ecotype *WS-4*) and *bot1-7* meristems. Membranes are labeled with FM4-64 (white) and *pBOUND>>GFP* expression is shown using the Fire lookup table in ImageJ. (**B**) Longitudinal sections through the middle of successive boundaries of the meristems presented in A (2 µm thick maximal projection of orthogonal views). Organ size (surface area as viewed from the top) is written in red for each stage. Note the delay in tissue folding and GFP signal expression in *bot1-7* when compared to the WT. The white line marks the outer surface of the SAM. (**C**) Quantification of the delay in curvature at the boundary in *bot1-7*: Folding angle is measured on orthogonal views and organ size is estimated from the measurement of surface area on top views. (**D**) The correlation between the folding angle of the boundary and the area of *pBOUND>>GFP* expression is maintained in *bot1-7* (both parameters are measured on orthogonal sections; WT: n = 130 from 5 SAM followed during a time lapse of 5 time points during 48 h, *bot1-7*: n = 79 from 3 SAM followed during a time lapse of 5 time points during 48 h). Values are displayed with a Student confidence interval ($\alpha = 0.05$) and compared using a bilateral Student test. Scale bars: 20 µm.

DOI: http://dx.doi.org/10.7554/eLife.07811.007

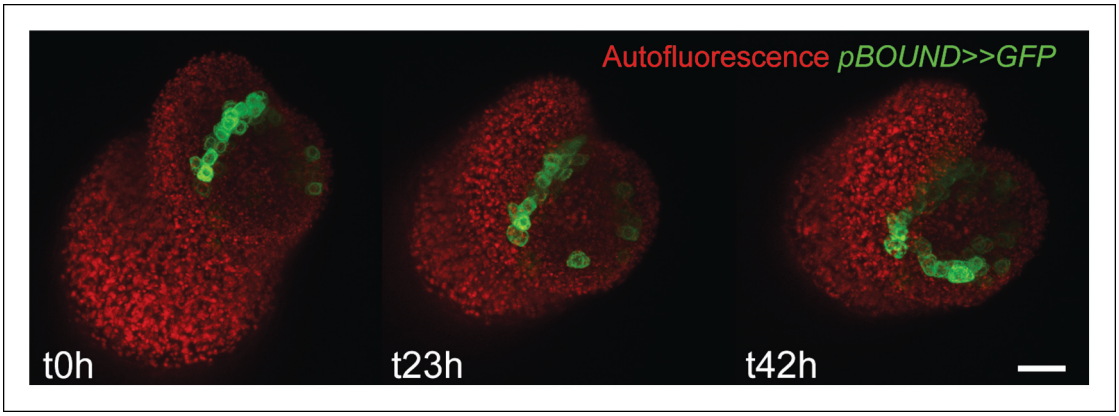

Figure 2—figure supplement 1. Time lapse of a *pBOUND>>GFP* meristem recovering from NPA treatment. Note the signal induction in old and new boundaries. Scale bar, 20 μm.
DOI: http://dx.doi.org/10.7554/eLife.07811.008

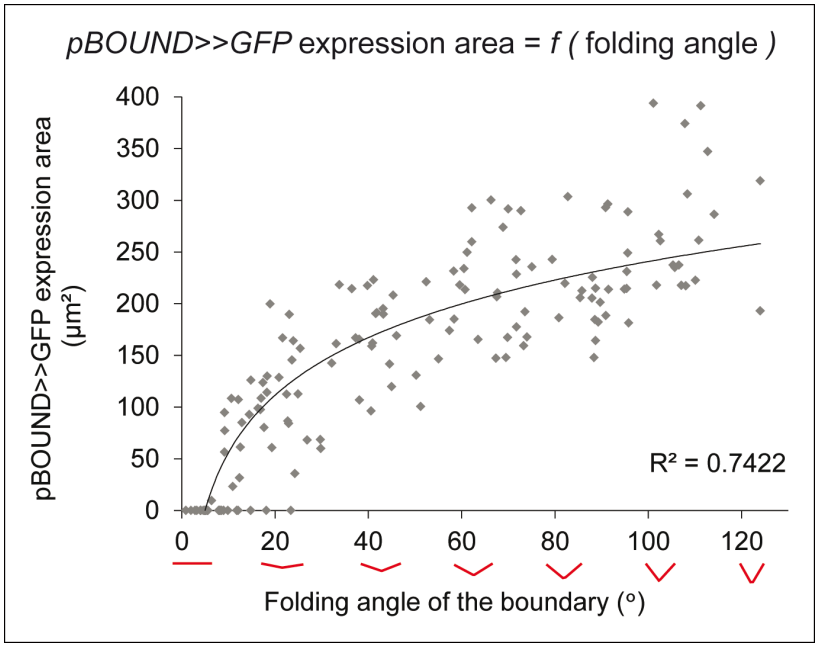

Figure 2—figure supplement 2. Correlation between pBOUND>>GFP expression area and tissue folding at the boundary. Quantitative correlation between the folding angle of the boundary and the area of *pBOUND>>GFP* expression on longitudinal sections from another independent time course as the one presented in ***Figure 2*** (n = 154, 5 meristems imaged 5 times over a time course of 48 hr).

DOI: http://dx.doi.org/10.7554/eLife.07811.009

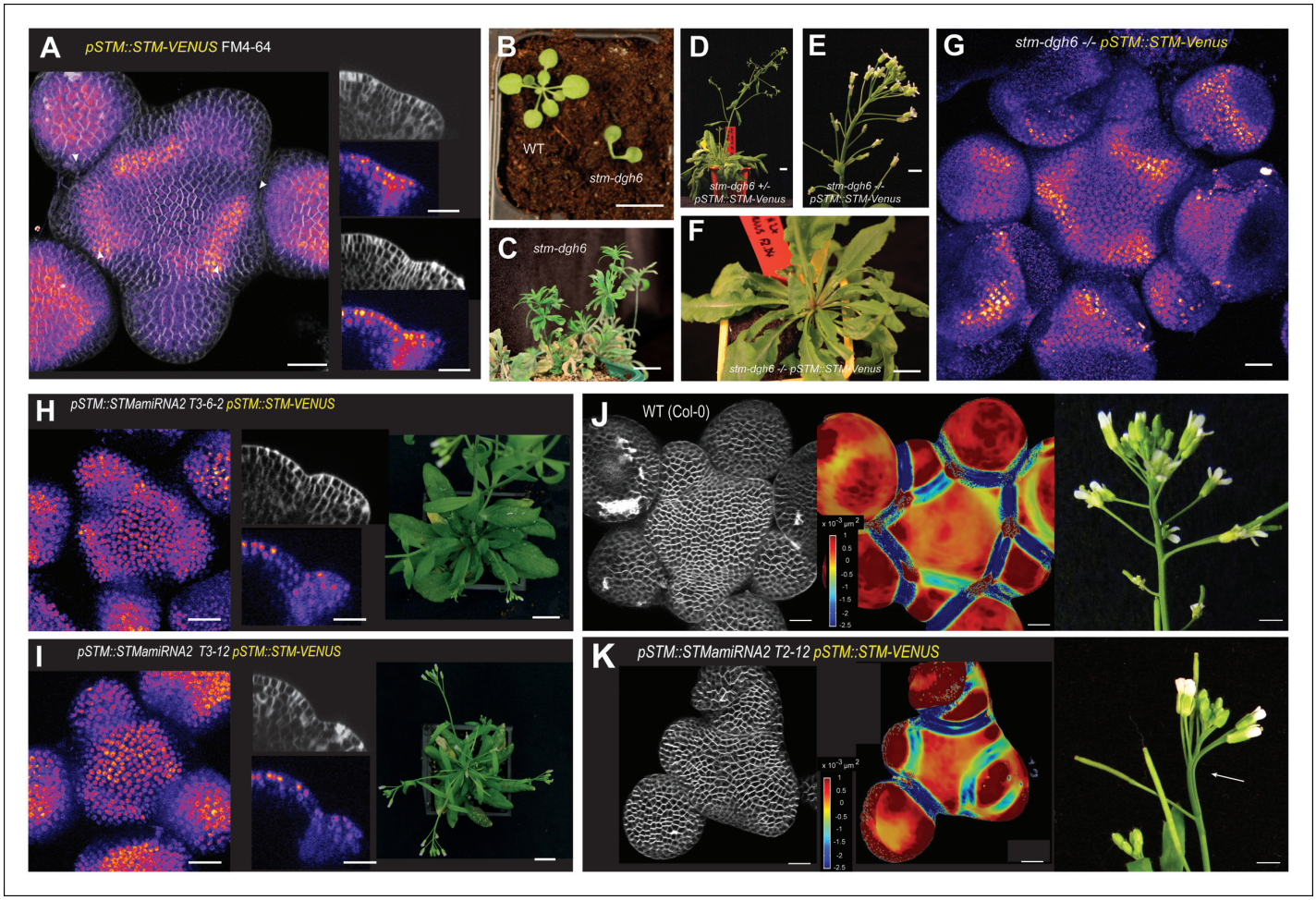

Figure 3. Organ separation requires *STM* expression at the boundary. (**A**) Representative expression pattern of the translational fusion *pSTM::STM-Venus* in a FM4-64 stained meristem showing an increased signal intensity in boundaries. Scale bar, 20 μm. (**B–F**) The translational fusion *pSTM::STM-Venus* partially rescues the phenotype of the strong mutant allele *stm-dgh6* (n = 5). (**B**) Phenotype of 3-week-old WT and *stm-dgh6* plants. Note the absence of postembryonic organs in the mutant. Scale bars, 1 cm. Aerial phenotype of 2-month old *stm-dgh6* plants. Scale bar, 1 cm. (**D**) Representative *stm-dgh6 pSTM::STM-Venus* plant. Scale bar, 1 cm. (**E**) Representative *stm-dgh6 pSTM::STM-Venus* inflorescence. Scale bar, 1 cm. (**F**) Representative *stm-dgh6 pSTM::STM-Venus* rosette. Scale bar, 1 cm. (**G**) Representative expression pattern of the translational fusion *pSTM::STM-Venus* in a *stm-dgh6* (-/-) meristem showing a similar expression pattern as in the WT. Scale bar, 20 μm. (**H, I**) Homogeneous expression pattern of the translational fusion *pSTM::STM-Venus* in two independent *pSTM::STMamiRNA* lines. Scale bar (microscopy), 20 μm. Scale bar (whole plant), 1 cm. (**J**) FM4-64 stained WT meristem (ecotype *Col-0*), Gaussian curvature extracted using the level set method and MorphoGraphX, Scale bar (microscopy), 20 μm. Scale bar (inflorescences), 1 cm. (**K**) FM4-64 stained *pSTM::STMamiRNA pSTM::STM-Venus* meristem, Gaussian curvature extracted using the level set method and MorphoGraphX. Scale bar, 20 μm. Boundaries do not scale to the reduced meristem size; inflorescence phenotype with fusion events. Scale bar, 1 cm.

DOI: http://dx.doi.org/10.7554/eLife.07811.010

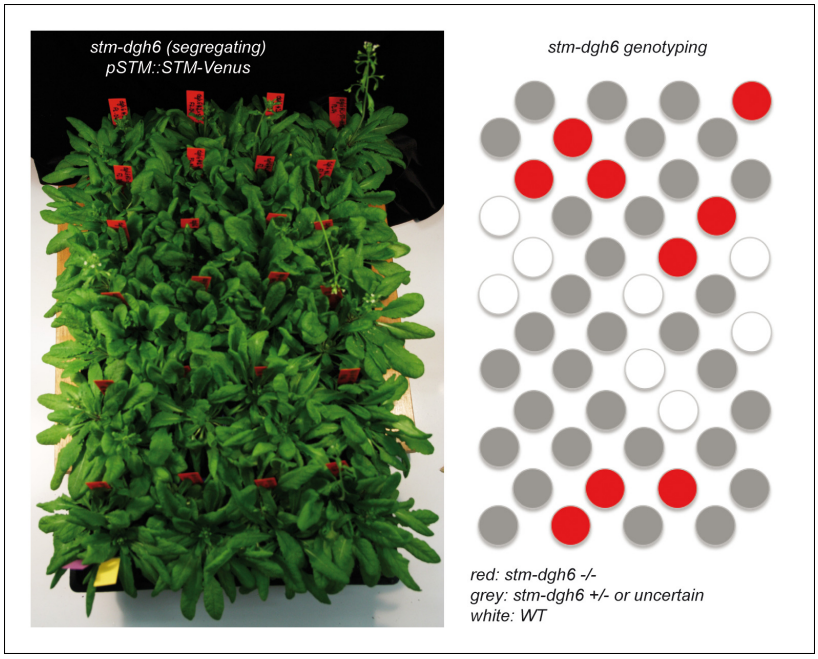

Figure 3—figure supplement 1. Molecular characterization of the *stm-dgh6 pSTM::STM-Venus*. (**A**) 48 *pSTM::STM-Venus* plants segregating the *stm-dgh6* mutation. (**B**) *stm-dgh6* genotyping of the plants shown in A. No obvious difference can be detected between the different lines.
DOI: http://dx.doi.org/10.7554/eLife.07811.011

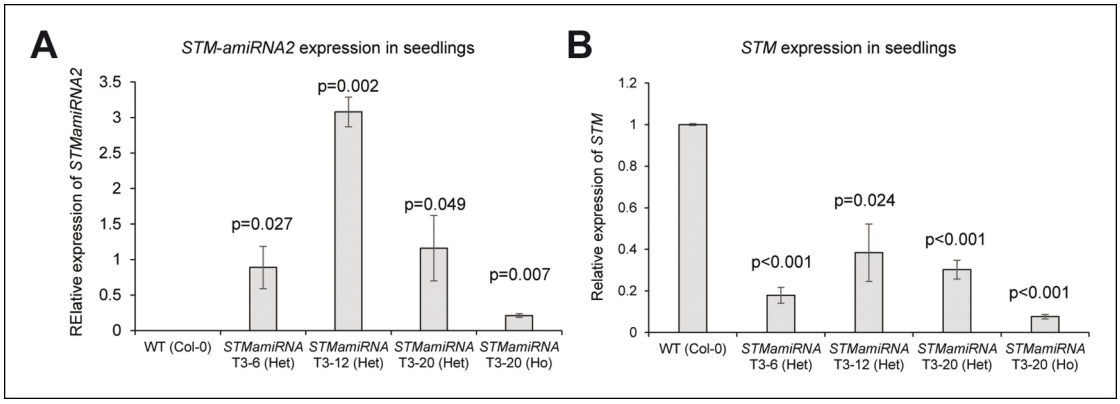

Figure 3—figure supplement 2. Molecular characterization of the *pSTM::STMamiRNA* lines. (**A**) *STMamiRNA* expression in 2-week-old seedlings by qPCR in three independent *pSTM::STMamiRNA* lines (see Material s and methods). Values are displayed with a Student confidence interval ($\alpha = 0.05$) and compared using a bilateral Student test. (**B**) *STM* expression in 2-weeks-old seedlings by qPCR in three independent *pSTM::STMamiRNA* lines, as in A.

DOI: http://dx.doi.org/10.7554/eLife.07811.012

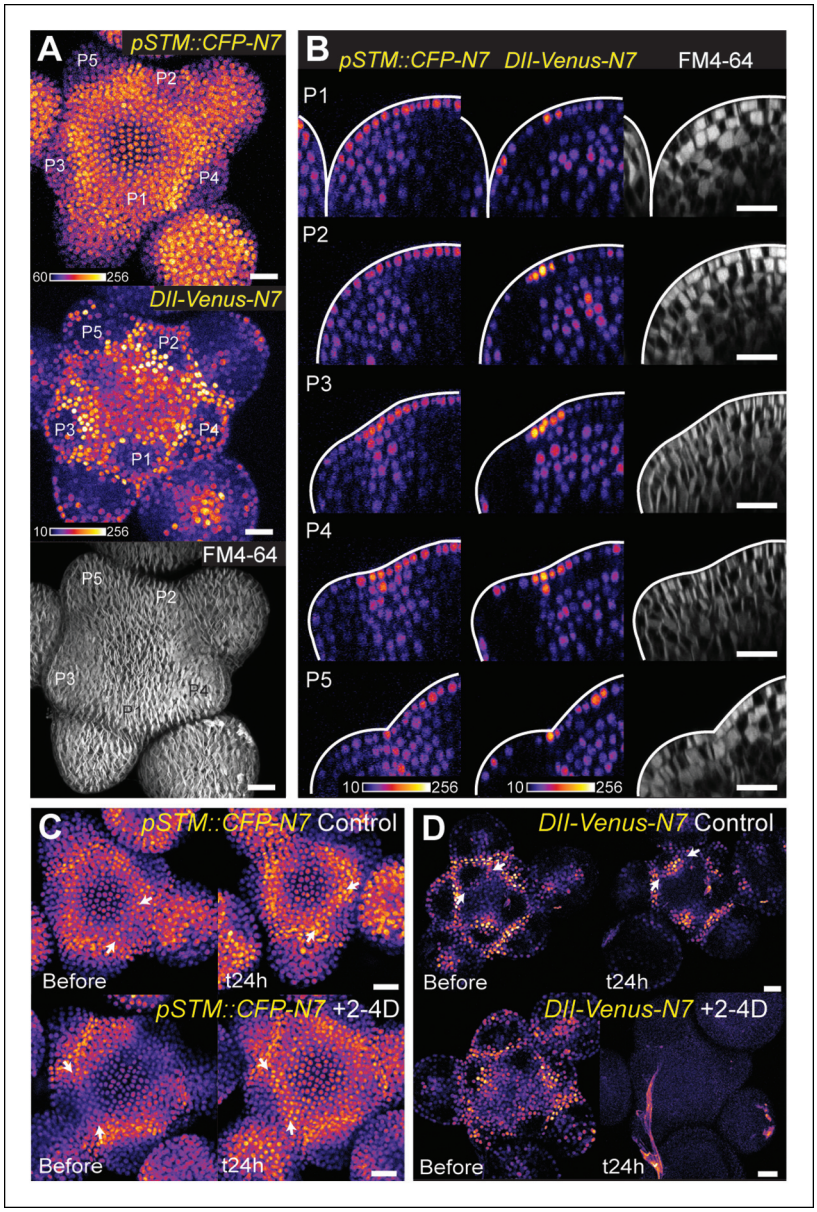

Figure 4. The DII-Venus and *pSTM::CFP-N7* signals largely overlap and can be uncoupled. (**A**) Projection of a representative meristem expressing both *pSTM::CFP-N7* and *DII-Venus-N7* and stained with FM4-64: both signals are induced in the boundary. (**B**) Orthogonal sections through the middle of the boundaries of the successive primordia of the SAM presented in showing an overlap of both signals, except in the L2 layer. (**C, D**) Overnight treatment with 10 μM of synthetic auxin 2,4-D on dissected meristems: (**C**) no effect on *pSTM-CFP* expression after 2,4-D application (Control: n = 3, 2-4D treatment: n = 3). White arrows point at new *CFP* signals in boundaries (**C and D**); (**D**) total degradation of *DII-Venus* after 2,4-D application (Control: n = 11, 2-4D treatment: n = 12). Scale bars, 20 μm.

DOI: http://dx.doi.org/10.7554/eLife.07811.013

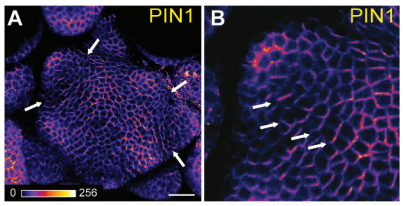

Figure 4—figure supplement 1. PIN1 localization in the SAM. Whole-mount PIN1 immunolocalization in the SAM (n = 6). (B) close-up from (**A**). White arrows point at boundaries where the polarity of PIN1 is strengthened and predicts an auxin depletion in this domain. Scale bars, 20 μm.

DOI: http://dx.doi.org/10.7554/eLife.07811.014

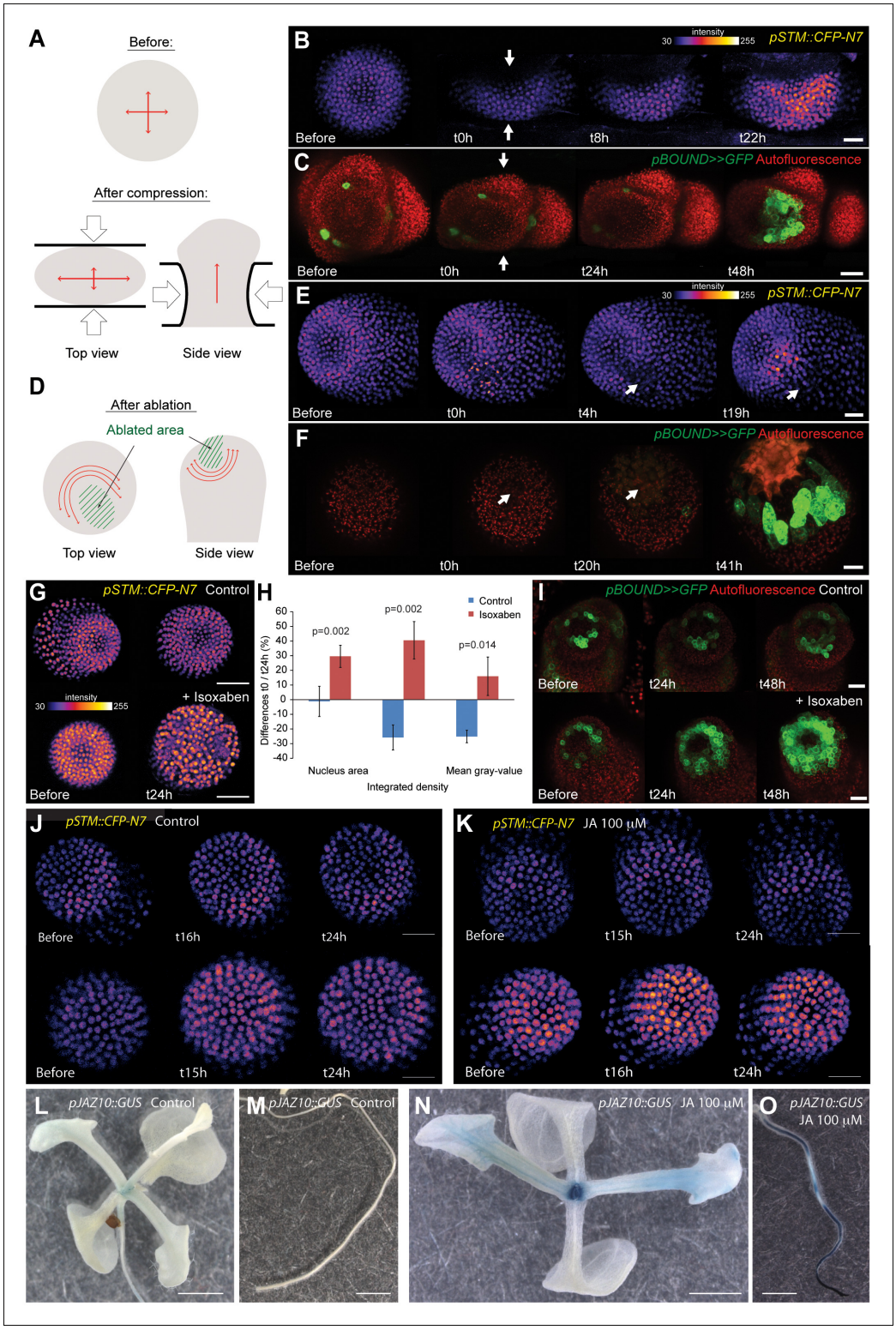

Figure 5. *STM* expression can be induced by mechanical perturbations. (**A to C**) Global compression of meristems with a microvice lead to an increase in *STM* expression (arrows indicate the direction of the compression). (**A**) Predicted impact of compression on the mechanical stress pattern. (**B**) *pSTM::CFP-N7* signal before and after compression in a representative meristem (n = 8). (**C**) *pBOUND>>GFP* signal before and after compression in a representative meristem (n = 11, red dots correspond to plast auto-fluorescence). (**D to F**) Ablation of a small number of cells leads to an increase in *STM* expression (white arrows indicate the site of ablation). (**D**) Predicted

Figure 5. continued on next page

Figure 5. Continued

impact of a local ablation on the mechanical stress pattern. (**E**) *pSTM::CFP-N7* signal before and after ablation with a needle (n > 30). (**F**) *pBOUND>>GFP* signal before and after ablation using a pulsed UV laser (n > 12, red dots correspond to plast auto-fluorescence). (**G and H**) Isoxaben treatment leads to an increase of *pSTM::CFP-N7* signal. (**G**) Representative *pSTM::CFP-N7* signal after overnight immersion in water with DMSO (upper panel) or in 10 μM isoxaben (lower panel). Note the increased nucleus size after isoxaben treatment, consistent with increased endoreduplication levels. (**H**) Quantifications: CFP signal intensity in 10 nuclei from the central zone of 6 isoxaben-treated meristems and 7 water-treated meristems. Values are displayed with a Student confidence interval (α = 0.05) and compared using a bilateral Student test. (**I**) Isoxaben treatment leads to an increase in *pBOUND>>GFP* signal (red dots correspond to plast auto-fluorescence). (**I**, left) Representative *pBOUND>>GFP* signal after overnight immersion in water (n = 10). (**I,** right) Representative *pBOUND>>GFP* signal after overnight immersion in 5 to 20 μM isoxaben (n = 20). Scale bars, 20 μm. (**J, K**) Jasmonate does not enhance *STM* promoter activity **(J)** *pSTM::CFP-N7* signal after prolonged incubation in water supplemented with 1/1000 V/V ethanol. **(K)** *pSTM::CFP-N7* signal after prolonged incubation in water supplemented with 100 μM jasmonate diluted in ethanol (1/1000 V/V). Scale bars, 20 μm. (**L-O**) Jasmonate enhances *pJAZ10* promoter activity. **(L, M)** Aerial part **(L)** and root **(M)** of 3 week old NPA grown seedlings. *pJAZ10::GUS* staining after overnight incubation in water supplemented with 1/1000 V/V ethanol (n = 8). (**N,O**) Aerial part (**N**) and root (**O**) of 3 week old NPA grown seedlings. *pJAZ10::GUS* staining after overnight incubation in water supplemented with 100 μM jasmonate diluted in ethanol (1/1000 V/V) (n = 14). Scale bars, 0.5 cm.

DOI: http://dx.doi.org/10.7554/eLife.07811.015

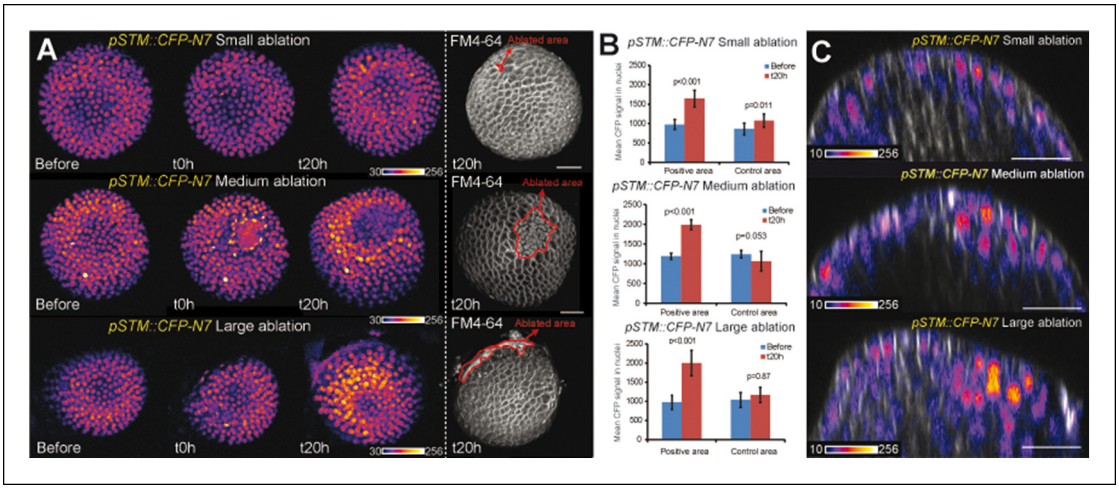

Figure 5—figure supplement 1. *pSTM::CFP-N7* induction after ablations of different sizes. (**A**) Z-projections of meristems expressing *pSTM::CFP-N7* and labeled with FM4-64 (white) before and after ablations of different sizes. (**B**) Quantification of the CFP signal intensity in 10 nuclei around the ablation site (positive area) or in the opposite side of the meristem (control area) of the three meristems presented in A. Values are displayed with a Student confidence interval ($\alpha = 0.05$) and compared using a bilateral Student test. (**C**) Longitudinal sections (5 µm thick maximal projections) of the ablated meristems presented in A, 20 hr after the ablations revealing that the induction of *pSTM::CFP-N7* roughly scales to the ablation size. Scale bars, 20 µm.

DOI: http://dx.doi.org/10.7554/eLife.07811.016

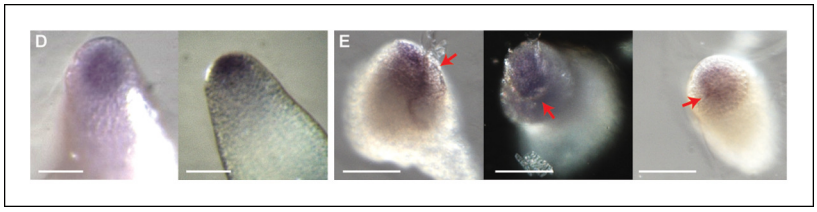

Figure 5—figure supplement 2. *STM* mRNA distribution after ablation in the SAM. (**A**) Whole mount in situ hybridizations using a *STM* probe in a SAM from WT NPA grown plants. (**B**) Whole mount in situ hybridizations using a *STM* probe in a SAM from WT NPA grown plants 24 hr (right and left panels) and 48 h (central panel) after ablation. Red arrows point at the ablation sites. Scale bars, 100 μm.

DOI: http://dx.doi.org/10.7554/eLife.07811.017

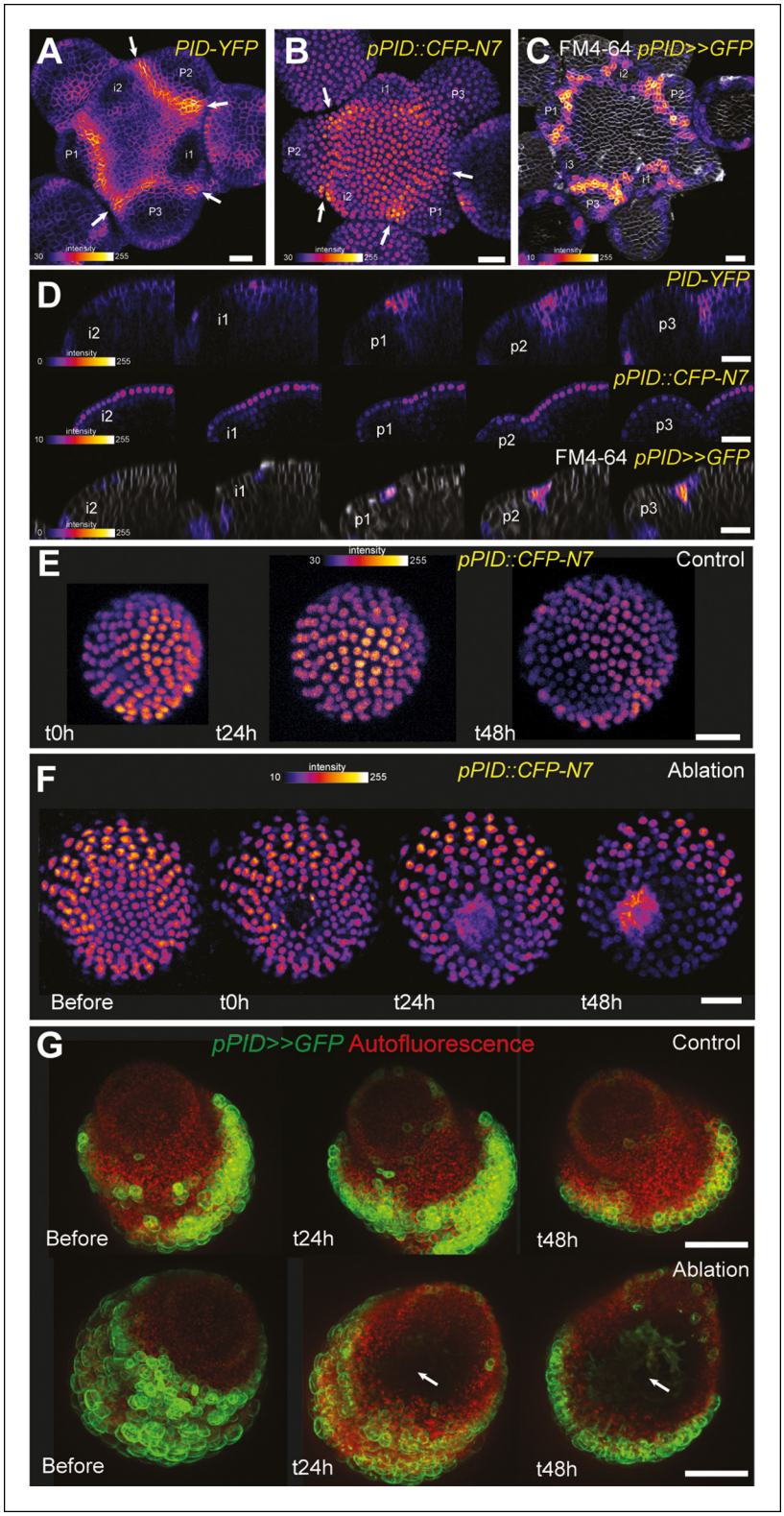

Figure 6. *PINOID* promoter activity is not affected by mechanical perturbations. (**A–C**) PINOID expression pattern in representative meristems: a higher expression of PINOID is observed in boundaries. (**A**) Expression pattern of the translational fusion *pPID::PID-YFP*. (**B**) Expression pattern of the transcriptional reporters *pPID::CFP-N7*. (**C**) Expression pattern of *pPID>>GFP*. (**D**) Orthogonal sections through the middle of the boundaries of the meristems presented in (**A–C**). (**E–F**) Time lapse of a representative meristems showing the absence of response of

Figure 6. continued on next page

Figure 6. Continued

pPID::CFP-N7 (**F**, n = 13) after ablation when compared to the control (**E**, n = 6). (**G**) Time lapse of a representative meristems showing the absence of response of *pBOUND>>GFP* after ablations (control n = 14, ablation n = 7). Scale bars, 20 μm.

DOI: http://dx.doi.org/10.7554/eLife.07811.022

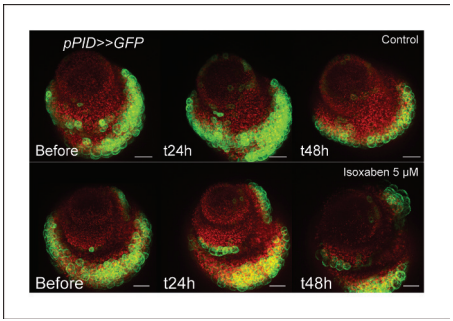

Figure 6—figure supplement 1. *pPID* is not significantly induced by isoxaben treatment. Overnight treatment with isoxaben does not lead to an induction of *pPID::GFP* expression, even 48 h after the first exposition to isoxaben. (Control, n = 14; isoxaben treatment, n = 11). Scale bars, 20 µm.
DOI: http://dx.doi.org/10.7554/eLife.07811.023

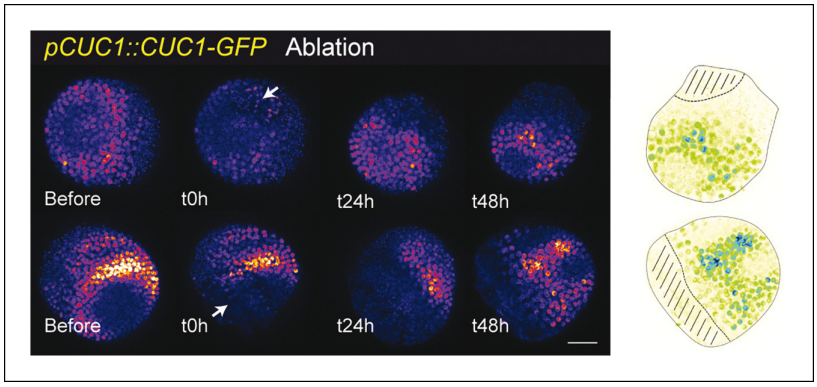

Figure 6—figure supplement 2. *pCUC1* is not significantly perturbed after an ablation in the SAM. *pCUC1::CUC1-GFP* expression after an ablation (arrow). No major changes are induced, and the pattern follows the organogenetic pattern instead of consolidating around the ablation site (n = 11). Scale bar, 20 μm. Drawings illustrate the last time points, with the hatched zone corresponding to the ablated zone.
DOI: http://dx.doi.org/10.7554/eLife.07811.024

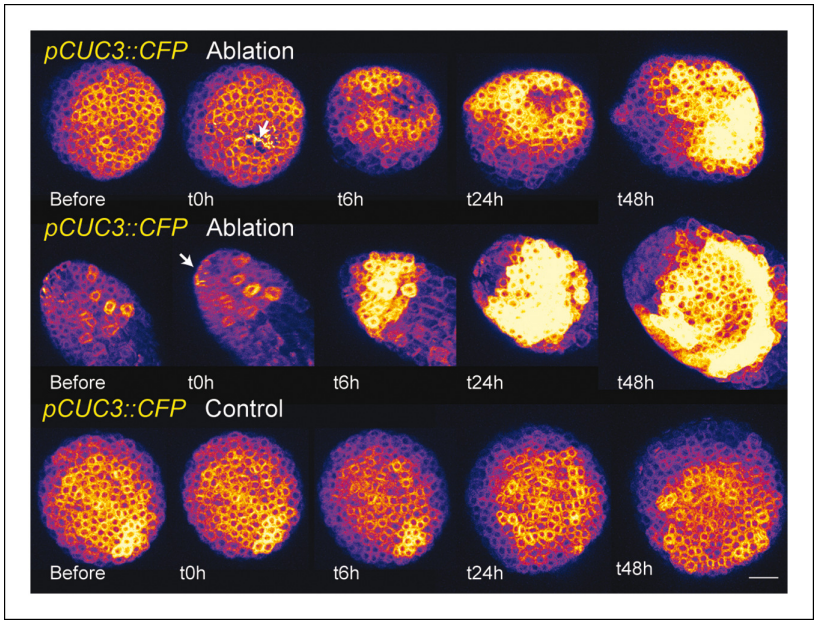

Figure 6—figure supplement 3. *pCUC3* is induced after an ablation in the SAM. *pCUC3::CFP* expression after an ablation. Note the steady induction, when compared to control (bottom line, n = 20). Scale bar, 20 μm.
DOI: http://dx.doi.org/10.7554/eLife.07811.025

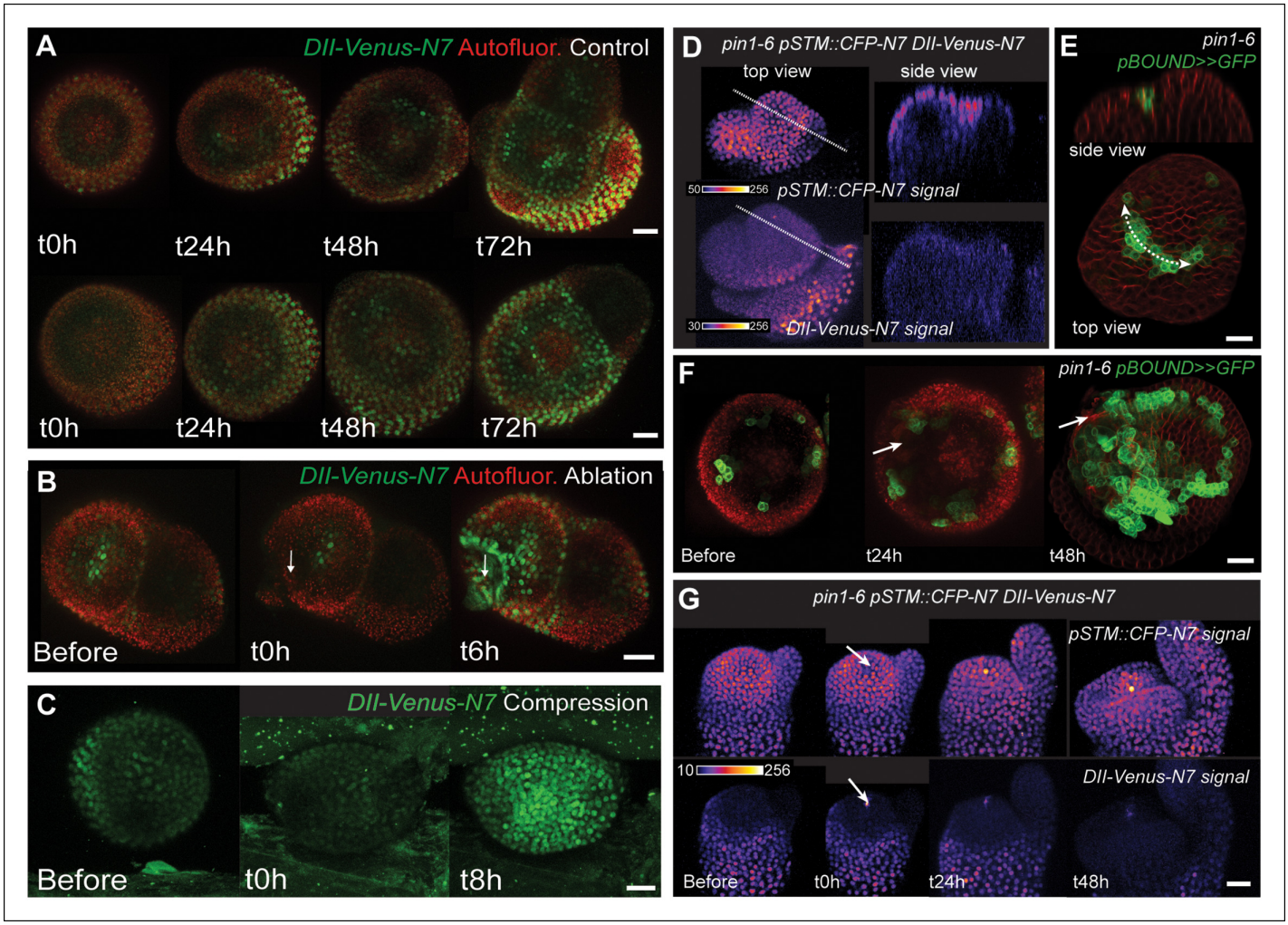

Figure 7. *STM* response to mechanical perturbations can be uncoupled from PIN1-dependent auxin distribution. (**A**) Time lapse of representative meristems from a NPA-grown plant and expressing DII-Venus. From t = h, the plants are not exposed to NPA anymore. (**B**) *DII-Venus-N7* signal increases after ablation: Time lapse of a representative meristems from a NPA-grown plant and expressing DII-Venus as in C, after ablation (Control n = 15, Ablation n = 21). (**C**) Representative DII-Venus signal before and after compression. An increased signal is usually detected after 4 to 8 hr after compression in the overall meristem (n = 10). (**D**) Representative *pin1-6* meristem expressing *DII-Venus-N7* and *pSTM::CFP-N7*: the presence of CFP signal at the pseudo-boundary does not correlate with DII-Venus-N7 signal anymore (n = 6). (**E**) Representative *pin1-6* meristem expressing *pBOUND>>GFP* showing the presence of GFP signal in a pseudo-boundary (n = 7). (**F**) Representative *pin1-6 pBOUND>>GFP* meristem after ablation: *pBOUND>>GFP* is induced around the site of ablation (n = 14). (**G**) Representative *pin1-6 DII-Venus-N7 pSTM::CFP-N7* meristem after ablation: *pSTM::CFP-N7* is induced around the site of ablation but *DII-Venus-N7* is not (n = 10). Scale bars, 20 μm.

DOI: http://dx.doi.org/10.7554/eLife.07811.026

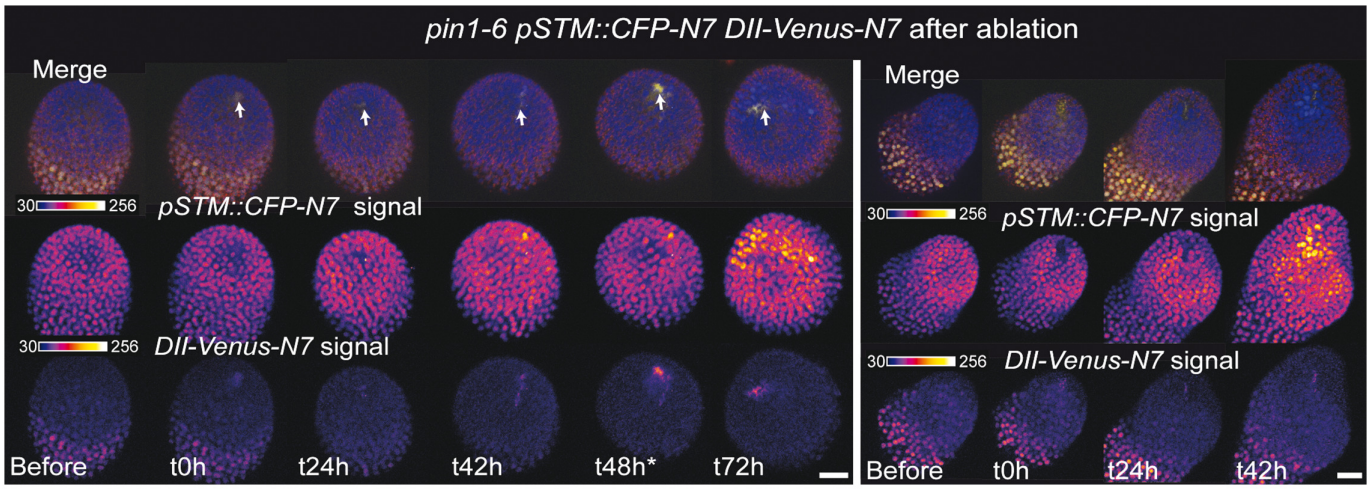

Figure 7—figure supplement 1. *pin1-6 DII-Venus-N7 pSTM::CFP-N7* meristem after an ablation in the SAM. Two representative *pin1-6 DII-Venus-N7 pSTM::CFP-N7* meristem after ablation (time-lapse): *pSTM::CFP-N7* is induced around the site of ablation but not *DII-Venus-N7* (n = 10).
DOI: http://dx.doi.org/10.7554/eLife.07811.027

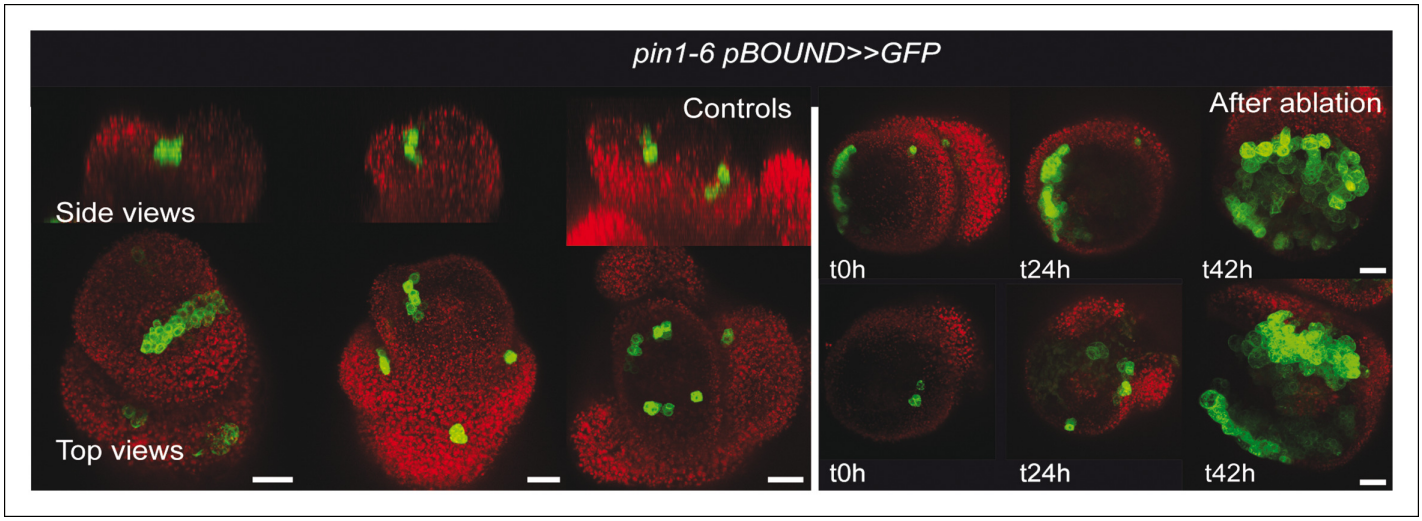

Figure 7—figure supplement 2. *pin1-6 pBOUND>>GFP* meristem after an ablation in the SAM. Representative *pin1-6* meristems expressing *pBOUND>>GFP* showing the presence of GFP signal in a pseudo-boundary (n = 7) and an induction of GFP signal after ablation (n = 14).
DOI: http://dx.doi.org/10.7554/eLife.07811.028

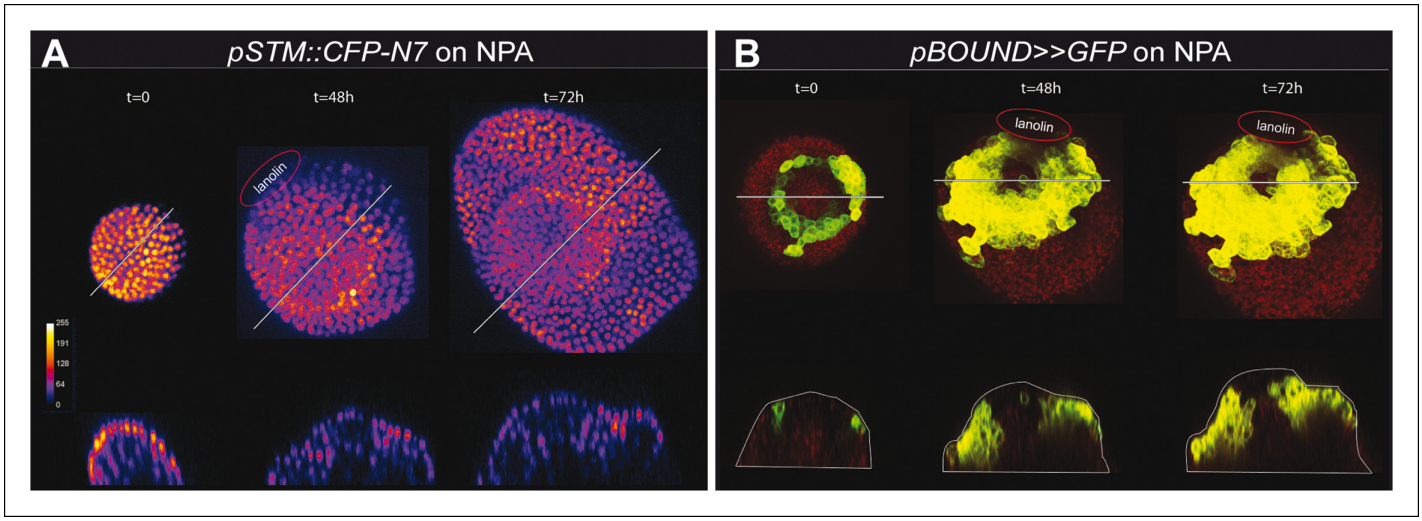

Figure 7—figure supplement 3. *STM* promoter activity during oryzalin-induced tissue folding in the presence of NPA. (**A**) Top and side views of a *pSTM::CFP-N7* meristem grown on NPA and maintained on NPA after the local application of the microtubule depolymerizing drug oryzalin. A bump is induced and a local increase in CFP signal is detected at the pseudo-boundary (n = 17/22). (**B**) Top and side views of a *pBOUND>>GFP* meristem grown on NPA and maintained on NPA after the local application of the microtubule depolymerizing drug oryzalin. A bump is induced and a local increase in GFP signal is detected at the pseudo-boundary (n = 20/21). Scale bars, 20 μm.

DOI: http://dx.doi.org/10.7554/eLife.07811.029